

# Development of Solar Energy Systems Based on High Performance Bulk and Film Thermoelectric Modules

S. Mamykin<sup>1,\*</sup>, I. Mamontova<sup>1</sup>, B. Dzundza<sup>2</sup>, Feng Gao<sup>3</sup>, R. Shneck<sup>4</sup> and Z. Dashevsky<sup>4,\*</sup>

<sup>1</sup>V. E. Lashkaryov Institute of Semiconductor Physics, National Academy of Sciences of Ukraine, 03028 Kyiv, Ukraine

<sup>2</sup>Department of Computer Technique, Vasyl Stefanyk Precarpathian National University, 76-000, Ivano-Frankivsk, Ukraine

<sup>3</sup>State Key Laboratory of Solidification Processing, School of Materials Science and Engineering, Northwestern Polytechnical University, Xi'an, 710072, China

<sup>4</sup>Department of Materials Engineering, Ben-Gurion University of the Negev, Beer-Sheva 84105, Israel

**Abstract:** Due to the increase in energy demand and depletion of natural resources, the development of energy harvesting technologies becomes very important. Thermoelectric devices, based on the direct conversion of heat into electrical energy, are being the essential part of cost-effective, environmental-friendly, and fuel-saving energy sources for power generation, temperature sensors, and thermal management. High reliability and long operation time of thermoelectric energy systems lead to their extensive use in space industry and gas pipe systems. Development and wide application of solar thermoelectric converters (generators) is mainly limited by relatively low thermoelectric conversion efficiency. In this work, we suggest for the first time to use direct conversion of solar energy by systems based on high-performance multistage thermoelectric modules operating in the temperature range of 300 - 900 K for creation of autonomic systems with electric power up to 500 W and electric efficiency up to 15 %. Furthermore, we developed film thermoelectric modules on thin flexible substrates with the figure of merit  $Z$  corresponding to that of bulk modules. Such film thermoelectric converters with output voltage of several volts and electric power of several microwatts can be used at micro-solar energy systems.

**Keywords:** Solar energy, Thermoelectric module, Figure of merit, Film thermoelectric microconverter.

## 1. INTRODUCTION

Growing demand for energy together with the need for non-polluting energy sources drives seek for novel types of electric converters, typically with direct energy conversion functionality [1-4]. The Sun is probably the most abundant and widespread source of energy on the Earth, which is available almost everywhere, albeit in different quantities. Sun is the source of almost any energy type, whether it is wind energy, fossil fuels, hydropower, biomass energy or even nuclear energy (if we consider the emergence of heavy elements such as uranium as a result of supernova explosions). Solar energy reaches the Earth's surface at a rate of 120 petawatts [5]. This means that all the solar energy received in one day can meet the needs of the whole world for more than 20 years [2]. Although our needs increase from year to year by a few percent (Figure 1), this renewable and inexhaustible energy source will be available during the entire period of existence of the Earth. Moreover, its power will grow in the long term due to the increase in the diameter of the Sun.

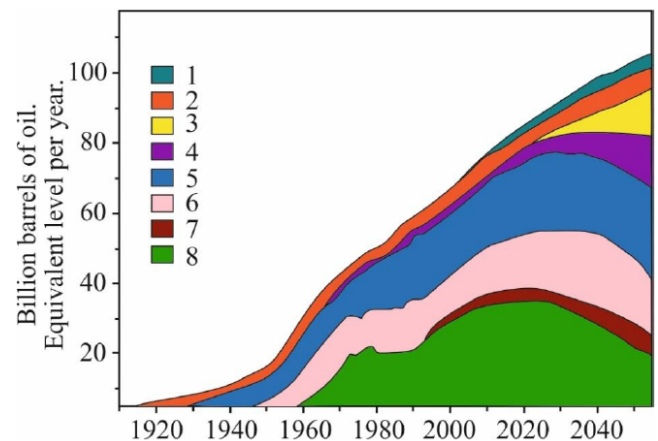


**Figure 1:** World energy demand and forecast [5].

1- biofuels, 2- hydroelectric, 3- solar, wind, geothermal, 4- nuclear electric, 5- coal, 6- natural gas, 7- shale/tar sands, 8- crude oil.

There are many ways to utilize solar energy: electricity generation, photochemistry, solar desalination and room temperature control. Among them, there is direct conversion of solar energy to electricity using photovoltaic cells and thermoelectric converters [2, 6]. The latter have an advantage, since they convert the energy of the entire solar spectrum through heating and creation of temperature gradient across the converter, while photovoltaic converters use

\*Address correspondence to this author at the V. E. Lashkaryov Institute of Semiconductor Physics, National Academy of Sciences of Ukraine, 03028 Kyiv, Ukraine; Tel: +38(044)525-60-10; E-mail: mamykin@isp.kiev.ua; zdashev@bgu.ac.il

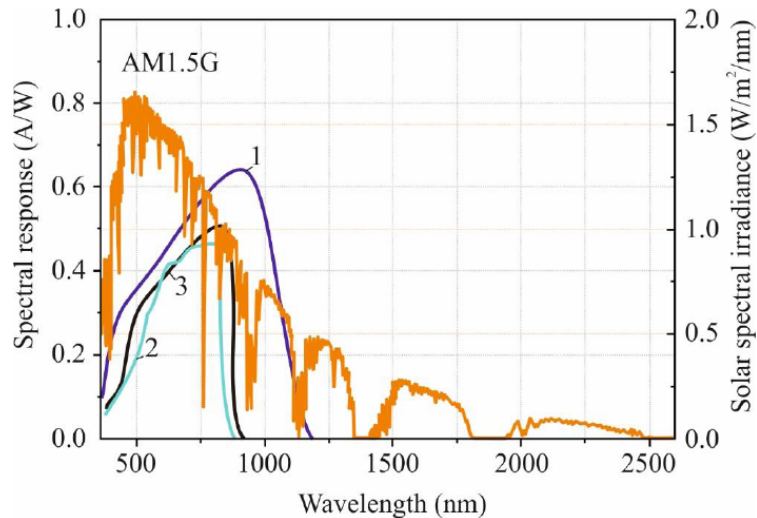


**Figure 2:** Spectral dependencies of solar power irradiance at AM1.5G conditions and response of the different efficient solar cells [7, 8]: 1 - Si, 2 - CdTe, 3 - GaAs.

only part of the spectrum (Figure 2) limited by the band gap energy of semiconductor they are made of. Moreover, waste heat, the source of which is not only the Sun but also cooling radiators of various devices as well as the surfaces of photoelectric converters that heat up during operation, can be also converted. Therefore, this way of collecting and converting solar energy into electricity will be widely applied having a profound impact on our society. Therefore, it has attracted the attention of researchers.

The efficiency of a thermoelectric generators (TEG) is the product of two terms, namely the Carnot and the thermoelectric efficiency. Respective equation is presented in [9].

Since the first suggestion by A.F. Ioffe semiconductors are considered as the best thermoelectric (TE) materials [9, 10]. At electron (hole) concentrations  $n(p) \sim 1 \times 10^{19} \text{ cm}^{-3}$  heat transport through semiconductors is mainly determined by phonons. At such carrier concentrations, the Fermi level  $E_F$  is close to the bottom of conduction band  $E_C$  for  $n$ -type semiconductors or to the top of valence band  $E_V$  for  $p$ -type semiconductors.

Prof. Z. Dashevsky showed three main parameters that determine the figure of merit  $Z$ . They are the effective mass of carriers ( $m_n^*$  in  $n$ -type and  $m_p^*$  in  $p$ -type semiconductors, respectively), the carrier mobility  $\mu$  and the phonon thermal conductivity  $k_L$ . The equation for  $Z$  as the function of these parameters is presented in [9, 11].

The values of  $ZT$  for different thermoelectric materials in the operating temperature range of 300 - 1200 K are published in [12-23]. Unfortunately, no thermoelectric material with optimal  $ZT$  over the wide temperature range is available now [9]. The legs of typical commercial thermoelectric generators are conventionally fabricated from one type of semiconductor materials [10].

Therefore, a way to increase the efficiency of thermoelectric converters is the creation of multilayer (multistage) thermoelectric unicouples. Such approach can provide optimal average values of figure of merit  $ZT$  over a wide temperature range.

## 2. TECHNOLOGY

### 2.1. Hot Pressing

The  $n$ - and  $p$ -type  $\text{Bi}_2\text{Te}_3$  based compounds were prepared using a hot pressing technique, which is a high-pressure (100 ton) powder metallurgy process for forming powder compact at high temperature of  $\sim 670$  K, sufficient to induce sintering (operating time  $\sim 0.5$  h) (Figure 3). The process was carried out in argon atmosphere [24-27]. Before hot pressing, the materials were synthesized in evacuated silica tubes. After that, the compounds were crushed into powder. The advantage of hot pressing technique is preparation of highly textured  $\text{Bi}_2\text{Te}_3$  based compounds [9]. These compounds are characterized by remarkable anisotropy due to their crystal structure, which is the basis for anisotropy of thermoelectric conversion efficiency.

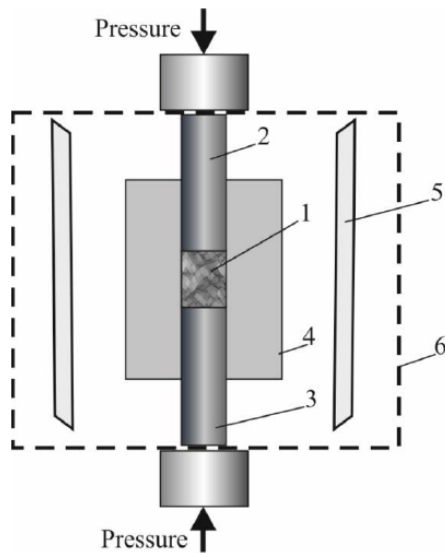


**Figure 3:** Schematic view of hot pressing set up.

1 - material powder, 2 - top plunger, 3 - bottom plunger, 4 - die, 5 - heating elements, 6 - vacuum chamber.

## 2.2. Spark Plasma Sintering (SPS) Technique

The  $n$ -type  $\text{Pb}_{1-x}\text{In}_x\text{Te}_{1-y}\text{In}_y$  and  $p$ -type  $\text{Ge}_{1-x}\text{Bi}_x\text{Te}$  were prepared using Spark Plasma Sintering (SPS) technique [28-32]. The powder was compacted at 1 GPa in a protective atmosphere at room temperature to form tablets 20 mm in diameter and 5 mm thick. Then the tablets were heated at a rate of 50 K/min and sintered by SPS at 870 K for 20 min in argon atmosphere under axial compressive stress of 60 MPa. The schematic view of SPS unit was presented in [9].

## 2.3. Flash Evaporation Technique for Preparation of Thin Thermoelectric Films

The  $p$ - $\text{Bi}_{0.5}\text{Sb}_{1.5}\text{Te}_3$  and  $n$ - $\text{PbTe}:\text{In}$  (I) films were deposited by flash evaporation technology, first proposed by Prof. Z. Dashevsky in 1974 [33]. A set up for obtaining films by this method is shown in Figure 4.  $\text{Bi}_{0.5}\text{Sb}_{1.5}\text{Te}_3$  or  $\text{PbTe}:\text{In}$  powder was introduced into the preheated quartz crucible (1) from a mechanically shaken powder vessel (7) [34, 35]. The evaporator was a quartz crucible (1) with a molybdenum wire heater (2) surrounded by a molybdenum heat screen (3). The powdered material was introduced into the crucible through a water-cooled channel (6). The substrate was heated by a substrate heater (5). All parts of the device were located in a chamber (8) under the vacuum of  $10^{-5}$  bar. The temperature of substrate during film preparation was  $T_s = 523 - 573$  K; the evaporation velocity was  $v_e = 0.1 \mu\text{m}/\text{min}$ . After the evaporation process, all films were annealed in the same

evaporation chamber at  $T_t = 623$  K for 0.5 h in pure argon atmosphere at the pressure of  $p = 0.9$  atm.

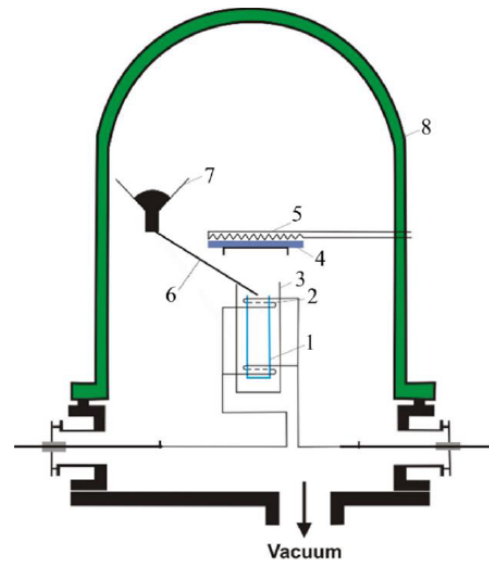


**Figure 4:** Schematic view of the flash evaporation set up.

1 - quartz crucible, 2 - crucible heater, 3 - heat shield, 4 - substrate, 5 - substrate heater, 6 - channel, 7 - powder vessel, 8 - vacuum chamber.

## 3. CHARACTERIZATION

### 3.1. Development of Measurement Set Up for Thermoelectric Module Characterization

Development and widespread use of thermoelectric generation as a user-friendly technology for direct energy conversion is mainly limited by small efficiency factors. Currently, the main efforts of scientists in the field of thermoelectricity are focused on increasing thermoelectric efficiency  $Z$  in wide range of operating temperatures (300-900 K). The main parameters that determine the quality of a thermoelectric material are the Seebeck coefficient, electrical conductivity and thermal conductivity. Moreover, electrical and operational characteristics, in particular internal resistance, generated current and voltage, thermoelectric power, heat capacity, etc are also crucial for the efficiency of thermoelectric power converters. All these parameters were measured by direct methods. A heat flow passed through a thermoelement due to the temperature gradient created between the heater and the cooler. A feature of the developed technique is use of two identical samples placed on both sides of the heater and cooled by identical water radiators. The measuring cell is schematically shown in Figure 5.

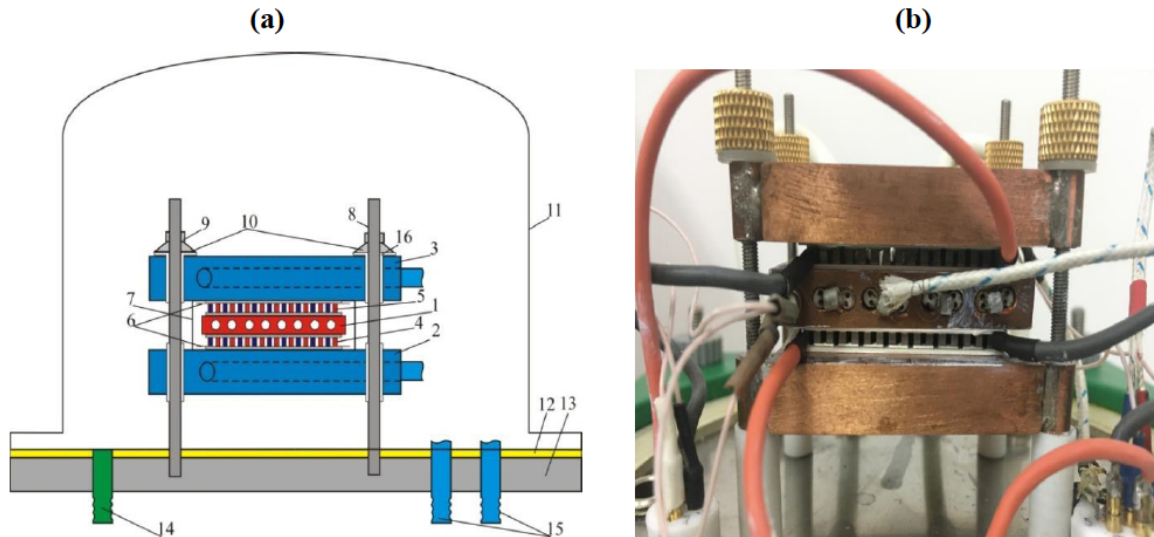


**Figure 5:** Schematic view of the measuring cell (a) and the photo of the measuring cell with installed thermoelectric elements (b).

1 - copper electric heater with thermocouple and 2, 3 - copper water radiator with thermocouple, 4, 5 - thermocouples or single samples of thermoelectric material, 6 - electrical contacts, 7 - heat shield, 8 - clamping pins, 9 - nuts, 10 - spring washers, 11 - vacuum cap, 12 - vacuum gasket, 13 - base, 14 - fitting for pumping, 15 - fittings for water supply and drainage, 16 - fluoroplastic insulation.

Cooling with running water made it possible to maintain stable temperature of cold junctions. To heat cylindrical or rectangular samples, a miniature low-power copper heater was made, which in combination with a tubular tantalum heat shield made it possible to significantly reduce parasitic heat losses, difficult to take into account.

To diagnose ready-made thermoelectric energy conversion modules with the size of  $40 \times 40 \text{ mm}^2$ , a rectangular copper heater with the size of  $40 \times 40 \times 8 \text{ mm}^3$  was made. It contacted the hot surfaces of the thermocouple through the thermal interface. The general view of the measuring cell is shown in Figure 5 b.

The design also provides the possibility of installing an additional heater on two additional threaded racks. This heater is installed at the level of the interface of the two radiators. This allows the study of film thermocouples, with the cold side clamped between two radiators, and the hot side is pressed by a copper plate to the additional heater.

All electrical contacts are routed through two sealed connectors located in the base. The set up supports up to 5 thermocouples. One thermocouple can be located in the heater, one more in the radiators, and two other can be drilled in the sample for additional control of heat fluxes. When the electrical properties of semiconductors are studied, such basic parameters as

electrical conductivity, Seebeck coefficient and thermoelectric power are measured.

The efficiency of TE uncouple (TE module) is defined as:

$$\eta = (P_1 + P_2) / Q, \quad (1)$$

where  $P_1$  and  $P_2$  are the electric power of the upper and the lower thermoelectric uncouple (or thermoelectric module), and  $Q$  is the heater power, respectively.

The temperature of the heater is changed in the range of 400 – 900 K with an accuracy of 2 %. The temperature of the radiators is controlled by a thermostat at  $\sim 300 \text{ K}$  with the accuracy of 1 %. The estimated accuracy of efficiency measurement is  $\sim 3 \%$ .

#### 4. HIGH-PERFORMANCE THERMOELECTRIC MATERIALS FOR APPLICATION IN ENERGY SYSTEMS

##### 4.1. Low-Temperature (300 - 600 K) Thermoelectric Materials Based on n-Type and p-Type $\text{Bi}_2\text{Te}_3$ Based Compounds

Bismuth telluride based compounds, namely *n*-type  $\text{Bi}_2\text{Te}_{3-x}\text{Se}_x$  and *p*-type  $\text{Bi}_{2-x}\text{Sb}_x\text{Te}_3$  solid solutions are the most effective thermoelectric materials operating at temperatures up to  $T_h \sim 600 \text{ K}$  [36-39].

Temperature dependences of Seebeck coefficient  $S$ , electrical conductivity  $\sigma$ , thermal conductivity  $\kappa$  and dimensionless figure of merit  $ZT$  in the temperature range of 300 - 600 K for  $p$ -type  $\text{Bi}_{0.5}\text{Sb}_{1.5}\text{Te}_3$  prepared by hot pressing were presented in [9].

The Seebeck coefficient  $S$  achieves maximum for all specimens and then decreases with increase in temperature. As shown in [9, 11], such behavior of  $S$  is related to appearance of electrons, which induce a negative value of  $S$  coefficient. In this case,  $S$  is determined as follows [11, 14]:

$$S = \frac{S_p\sigma_p + S_n\sigma_n}{\sigma_n + \sigma_p} \quad (2)$$

where indices  $n$  and  $p$  describe parameters for electrons and holes, respectively.

The electron mobility is higher than the hole one [11]. The electron concentration increases exponentially with temperature. In this case, we observe the sharp decrease of  $S$ . According to Eq. 2, Seebeck coefficient becomes anisotropic at high temperatures due to presence of opposite-sign charge carriers. As shown in [11], the negative effect of minority charge carriers is minimized in crystals with the orientation parallel to the axis  $C$ . At  $T > 500$  K, it results in higher values of the dimensionless figure of merit  $ZT$  for samples with the orientation parallel to this axis [11, 14].

Temperature dependence of Seebeck coefficient  $S$ , electrical conductivity  $\sigma$ , thermal conductivity  $\kappa$  and dimensionless figure of merit  $ZT$  in the temperature range of 300 - 600 K for  $n$ -type  $\text{Bi}_2\text{Te}_{3-x}\text{Se}_x$  samples prepared by hot pressing were presented in [9]. Such temperature behavior of  $S$ ,  $\sigma$ , and  $\kappa$  defines the maximum value of  $ZT \sim 1.2$  for the optimal composition of  $\text{Bi}_2\text{Te}_{2.7}\text{Se}_{0.3}$  solid solution with electron concentration  $n \sim 5 \times 10^{19} \text{ cm}^{-3}$  and  $S \approx -165 \text{ } \mu\text{V/K}$  at  $T \sim 300$  K. Consequently, the best TE material for  $n$ -type legs in thermoelectric low temperature converters is hot-pressed  $\text{Sb}_{1.3}$ -doped  $n$ - $\text{Bi}_2\text{Te}_{2.7}\text{Se}_{0.3}$  alloy.

#### 4.2. Middle Temperature (600 - 900 K) $n$ -type Thermoelectric Materials Based on PbTe Semiconductor Compound

The maximal value of the figure of merit  $Z$  as a function of electron density depends on the location of Fermi level  $E_F$  relative to the bottom of the conduction band  $E_C$ . It was shown that indium dopant in PbTe makes optimal the location of Fermi level by creation of

indium quasi local level in the conduction band. This leads to so-called pinning of Fermi level [40-43]. The indium level is the source of electrons which mitigate the influence of minority carriers (holes). This effect makes the average figure of merit  $(ZT)_{av}$  significantly higher over a wide temperature range. Additional improvement of  $(ZT)_{av}$  was achieved by co-doping PbTe with iodine, which is a well-known donor impurity for this material [44].

The temperature dependences of Seebeck coefficient, electrical conductivity, thermal conductivity and the dimensionless figure of merit  $ZT$  in the temperature range of 600 - 900 K for  $n$ -type  $\text{Pb}_{1-x}\text{In}_x\text{Te}_{1-y}\text{I}_y$  specimens prepared by SPS were presented in [9]. The maximum value of  $ZT$  for  $\text{Pb}_{0.999}\text{In}_{0.001}\text{Te}_{0.999}\text{I}_{0.001}$  was close to 1.3 at  $T = 750$  K, which is one of the highest values of  $ZT$  for  $n$ -type PbTe.

#### 4.3. Middle Temperature (600 - 900 K) $p$ -type Thermoelectric Materials Based on GeTe Compound

The  $p$ -type thermoelectric was based on GeTe semiconductor compound doped by Bi up to 5 atomic %. This enabled to decrease significantly the hole concentration to the optimal value from the point of view of TE efficiency ( $ZT$ ) [31]. On the other hand, this TE material has satisfactory mechanical characteristics, in contrast with high-efficiency  $p$ -type PbTe [45-48]. This property is very important for application in thermoelectric energy modules [49-51].

Temperature dependences of Seebeck coefficient, electrical conductivity, thermal conductivity and the dimensionless figure of merit  $ZT$  for  $p$ -type  $\text{Ge}_{1-x-y}\text{Bi}_x\text{Pb}_y\text{Te}$  prepared by SPS in the temperature range of 600 - 900 K were presented in [9].

The  $\text{Ge}_{0.96}\text{Bi}_{0.04}\text{Te}$  specimen has the lowest value of  $\kappa \approx 2 \text{ W/mK}$  at 600 K, which is more than twice less than that for GeTe specimen. This trend is observed up to  $T = 900$  K. The dimensionless figure of merit  $ZT$  for  $\text{Ge}_{0.96}\text{Bi}_{0.04}\text{Te}$  specimen reaches the value of  $\sim 2.0$  at  $T = 700$  K and remains virtually constant up to 900 K. This value is more than twice the value of  $ZT$  for pristine GeTe. The average thermoelectric figure of merit for  $\text{Ge}_{0.96}\text{Bi}_{0.04}\text{Te}$  specimen  $(ZT)_{av} \sim 1.3$  has been obtained for the operating temperature difference  $\Delta T = 300$  K ( $T_c = 900$  K,  $T_h = 600$  K). For comparison, the thermoelectric properties of a high-performance  $p$ -type  $\text{Pb}_{0.94}\text{TI}_{0.02}\text{Na}_{0.002}\text{Te}$  prepared by SPS [47] demonstrate higher value of  $ZT$  than for the  $\text{Ge}_{0.96}\text{Bi}_{0.04}\text{Te}$  specimen.

## 5. APPLICATIONS

### 5.1. Thermoelectric Module

To obtain maximum TE efficiency, we propose to fabricate composite TE modules (TEMs) from multilayer unicouples designed for given temperature gradients, following the suggestion of Prof. Z. Dashevsky [31]. Each stage should be made of a different material layer. Each material was selected such that its ZT is maximal in the temperature range prevailing in the corresponding stage.

The structure and the composition of a multilayer (multistage) TE uncouple designed for operation in the temperature range of 300 – 900 K are presented in Figure 6. The first layer material was prepared from low-temperature TE materials (the temperature interval is 300 – 600 K) based on *n*-type and *p*-type  $\text{Bi}_2\text{Te}_3$  fabricated by hot pressing (layers 2 and 5). The second and the third layer materials for *n*-type thermoelectric leg were PbTe based compounds, namely PbTe doped by iodine (3) and  $\text{Pb}_{0.999}\text{InTe}_{0.999}\text{I}_{0.001}$  (4). The second layer of *p*-type thermoelectric leg was prepared from  $\text{Ge}_{1-x}\text{Bi}_x\text{Te}$  (7) by Spark Plasma Sintering (SPS). The metallic contacts were fabricated by hot pressing, namely the cobalt layer (1) as the contact between *n*-type and *p*-type legs on the cold side and the iron layer (9) as the contact between *n*-type and *p*-type legs on the hot side. A thin layer of heavy doped *p*-type SnTe (8) prepared by SPS was used for decreasing contact resistance for *p*-leg on the hot side.

Several multi-layer unicouples were fabricated, and their efficiency was measured using the set up described in subsection 3.1. The experiments showed

that the energy conversion efficiency reached a high value of ~ 14-15 % when operated between the hot temperature  $T_h = 900$  K and at cold temperature  $T_c = 320$  K.

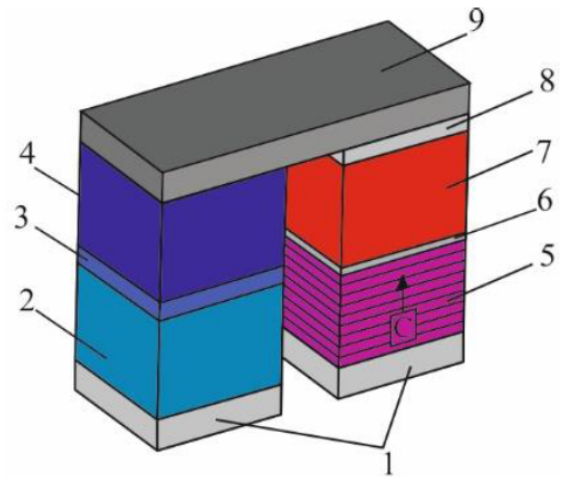


**Figure 6:** Schematic view of multilayer thermoelectric generator uncouple (for the temperature range  $T_c = 320$  K and  $T_h = 900$  K).

1 - metallic contact from Co + 6 wt % Bi prepared by hot pressing. 2 - *n*-type TE layer prepared by hot pressing of  $n\text{-Bi}_{2.7}\text{Se}_{0.3}\text{Te}_3$ . 3 - *n*-type TE layer made by SPS of  $n\text{-Pb}_{0.999}\text{InTe}_{0.999}\text{I}_{0.001}$ . 4 - *n*-type TE layer prepared by SPS of  $n\text{-Pb}_{0.999}\text{InTe}_{0.999}\text{I}_{0.001}$ . 5 - *p*-type TE layer prepared by hot pressing of  $p\text{-Bi}_{0.5}\text{Sb}_{1.5}\text{Te}_3$ , oriented along the axis C. 6 - thin anti-diffusion layer prepared by hot pressing of  $\text{CoGe}_2$  compound. 7 - *p*-type TE layer prepared by SPS of  $p\text{-Ge}_{0.96}\text{Bi}_{0.04}\text{Te}$ . 8 - thin heavily doped *p*-type SnTe layer prepared by SPS for improving ohmic contact. 9 - Fe metal contact on the hot side prepared by hot pressing.

Fabrication of the proposed thermoelectric module (TEM) (Figure 7) may include the following steps:

1. Assembly of the developed TE unicouples into an aluminum cassette (Figure 7a).

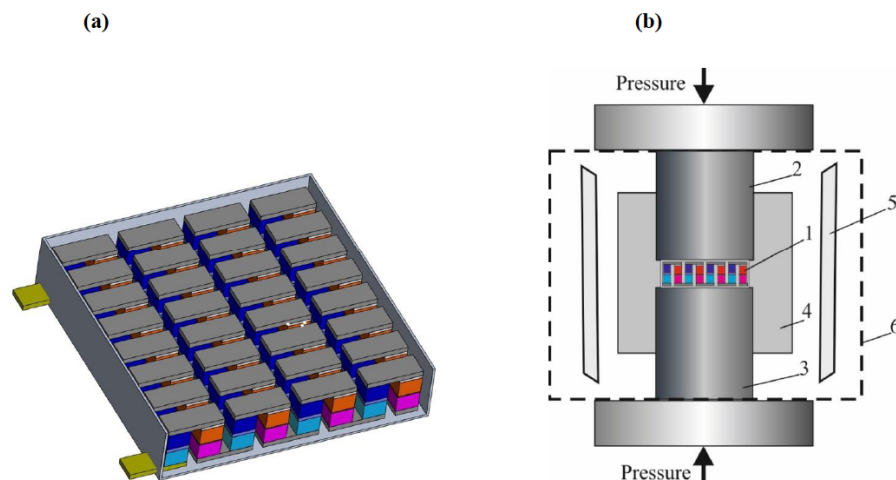


**Figure 7:** Assembly of the thermoelectric unicouples into an aluminum cassette (a). Sintering process (b).

**Table 1: Characteristics of Thermoelectric Module**

Dimensions, mm-mm-mm	Quantity of uncouples	Hot temperature, $T_h$ , K	Cold temperature, $T_c$ , K	Outside voltage $U$ , V	Current $I$ , A	Electric power $P_e$ , W
100-20-10	50	900	300-320	4	20	80

2. Sintering the cassette by hot pressing (during 0.5 h at  $T_h = 700$  K in argon atmosphere) (Figure 7b).

3. Formation of a chain of thermoelements connected in series.

4. Assembly of the TE module in a protective case of stainless steel thin sheet (argon atmosphere).

## 5.2. Solar Thermoelectric System (STES)

The first design of gas thermoelectric generator with electric power of 170 W and efficiency  $\sim 8\%$  based on multistage thermoelectric modules ( $T_h = 800$  K,  $T_c = 350$  K) was developed in the laboratory of Prof. Z. Dashevsky in 1993. These TEGs provided a high reliability and long operative time of  $\sim 25$  years [52].

The schematic view of a novel Solar Thermoelectric System (STES) is shown in Figure 8. Solar radiation is collected by the light receiver (1) with the tracking system (2) (heliostat) and directed to the absorber (3). Heat is accumulated in the thermal storage part (4) of STES in the phase change material, the melting temperature of which is close to the optimal operating temperature of the thermoelectric module (TEM) (6). Part of the thermal energy (up to 15%) is converted into electrical energy due to the difference  $\Delta T$  between the temperatures of the solar absorber (3) and radiators (7) on the cold side of the TEM. The cold part of the TEM is in contact with the radiator (7) equipped with the heat pipes (8) [53] to intensify the heat flow and direct it to the external radiators (9). In a conventional TEM, cooling radiators dissipate most of the thermal energy into the environment [54] due to convection and irradiation. Here, a special type of photonic radiative cooler [55-58] with enhanced radiative part is proposed to use.

### 5.2a. Light Collector

The solar collector is a Fresnel lens [59] with a Sun tracking system - a heliostat [60]. Its main features are that it is a thin plastic sheet embossed with concentric grooves having triangular profile. The area of such lens is calculated from the operating power of TEMs and for 5 kW it should be about  $5\div 6$  m<sup>2</sup>. Such collector has simple design, high accuracy, low weight and cost. The

low weight combined with the heliostat, also ensures high tracking accuracy when small motors and drive mechanisms are used.

Sun tracking applies polar coordinate system (the same basic mechanism as in a watch) for easy and accurate tracking. In addition, the unique design, combining the main axes of movement with the optical axis, allows directing concentrated solar radiation to a stationary receiver with a small round window.

A design of the type of hollow integrating sphere made of a low emissivity material (e.g., stainless steel or molybdenum) is proposed for the receiver of solar radiation. The surface of the sphere can be optionally covered with a heat-resistant light-absorbing material such as carbon black or carbon nanotubes [61]. Such surface itself absorbs well solar radiation due to microroughness. Moreover, reflected and scattered energy falls on other parts of the sphere, where it is additionally absorbed. The energy loss in such receiver is caused by only a small part of the radiation reflected and back out through the small receiving window of the sphere, which can be additionally covered by quartz window with antireflection coating [62]. Such window transmits solar light and reflect back low energy photons coming out from the heated sphere thus reducing solar energy loss.

### 5.2b. Thermal Energy Storage

The thermal storage (Figure 8) is based on a phase change material (PCM) with the latent heat of fusion used for energy storage. A solar receiver (3) is integrated into the storage vessel (4). This is done in order to ensure even absorption and to reduce thermal and hydrostatic loads (i.e. formation of local liquid pockets where high pressure may develop). The energy absorbed by such sphere makes PCM in the accumulator of the system heat and melt. Such battery uses the accumulated energy of phase transition to maintain the temperature of the hot end of the thermal converter to generate electricity during the dark part of the day. Current design proposes to use Al with melting point around 923 K as PCM. Al is non-toxic, environmentally harmless and readily available. Moreover, it has relatively high heat of fusion, ensuring

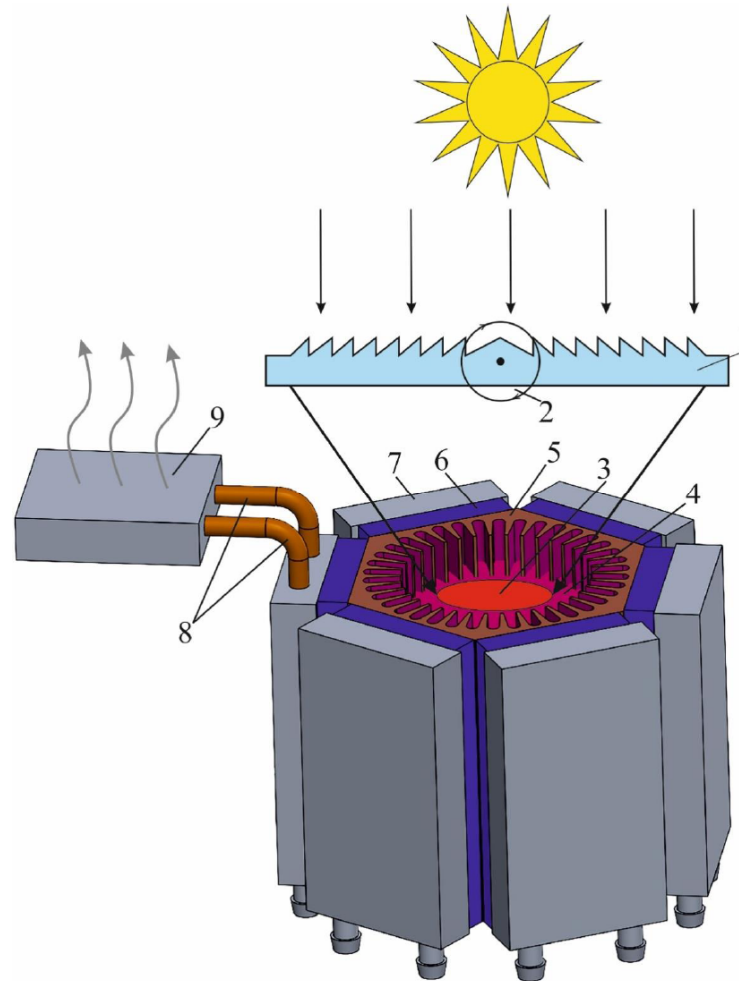


**Figure 8:** Schematic view of Solar Thermolectric System (STES).

1 - Fresnel lens. 2 - heliostat. 3 - solar receiver input (black body). 4 - thermal storage (Al alloy). 5 - heat exchanger. 6 - thermoelectric module (TEM). 7 - heat sink with heat pipes. 8 - heat pipes. 9 - photonic radiative cooler [55].

high storage density (400 Joules per gram). Finally, the melting temperature of Al can be tuned to 900 K by alloying with Cu, which is appropriate for the intended optimal high-end temperature of the system.

To roughly estimate the weight of Al needed to save thermal energy in the form of the energy of melting for the system with heat power  $Q = 5$  kW, we have to divide the collected energy during 12 hours of day time by the Al specific heat of fusion  $h=10.79$  kJ/mol and multiply by the Al molar mass  $M=26.98$  g/mol. The resulting weight of Al is about 540 kg.

### 5.2c. Thermoelectric Power Unit (TPU)

A schematic view of a TPU is presented in Figure 8. When it is considered to apply within an autonomous solar energy converter, it can be classified from the point of view of capacity, energy quality, operating temperature, location and utilization of heat. The temperature of heat exchanger (5) connected with TPU

is stable at about 900 K. Conceptual design of TPU was produced for heat exchanger (5) by square  $F = 1$  m<sup>2</sup> and heat power  $Q = 5$  kW. TPU consists of 6 TEMs (6) connected electrically in series and thermally in parallel. The cold side of each TEM is connected to the heat sink (7) equipped with heat pipes (8) [53]. The coolant in heat pipes is acetone solution at the temperature of 310 K.

Heat pipes intensify heat flow and direct it to external radiators (9) of photonic radiative cooler of a special type [55] with enhanced radiative part. The enhanced radiative cooling at the ambient air temperature under direct sunlight was experimentally demonstrated. Such thermal emitter reflects 97 % of incident sunlight while emitting strongly and selectively in the atmospheric transparency window of  $8\div 13$   $\mu\text{m}$ . Under direct sunlight with the power exceeding 850 watts per square meter, the photonic radiative cooler cools to around 5 K below ambient air temperature and

has a cooling power of 40.1 watts per square meter at ambient air temperature.

We expect that the prototype of such hybrid system can produce ~ 400- 500 W of electrical energy. The rest of thermal energy can be potentially used for domestic heating and hot water supply. The advantage of such system is high stability without operative service during about one year and long life time not less than ~20 - 25 years.

## 6. DEVELOPMENT OF HIGH-PERFORMANCE FILM THERMOELECTRIC MODULE FOR SOLAR APPLICATIONS

Presently, micro-energy converters for energy harvesting are more useful than standard electrical batteries. They have become realizable due to drastic decrease in power consumption of electronic components caused by advances in the field of electric energy storage, miniaturization, and optimization [63-71]. These films were fabricated by co-evaporation, molecular beam epitaxy, hot wall technique, magnetron sputtering and pulsed laser deposition [34]. However, high value of the figure of merit  $Z$  for  $\text{Bi}_2\text{Te}_3$ -based films comparable to that for bulk crystals ( $Z \sim 3 \times 10^{-3} \text{ K}^{-1}$ )

[11] was not achievable for a long time. Recently, the high value of  $Z \approx 3 \times 10^{-3} \text{ K}^{-1}$  at  $T = 300 \text{ K}$  for  $p$ -type  $\text{Bi}_{0.5}\text{Sb}_{1.5}\text{Te}_3$  films was obtained in the laboratory of Prof. Z. Dashevsky [34].

For film preparation, thin polyimide substrate with the thickness of ~ 10  $\mu\text{m}$  was used to minimize negative heat wastes. The benefits of polyimide material are the extremely low thermal conductivity (~3.5  $\text{Wcm}^{-1}\text{K}^{-1}$ ) and high flexibility [72]. Use of a flexible polyimide substrate and perforation cuts between  $p$ - and  $n$ -legs allowed us to develop a compact (packaged) design of Film Thermoelectric Module (FTEM).

### 6.1. Thermoelectric Properties

All  $p$ -type ( $\text{Bi}_{0.5}\text{Sb}_{1.5}\text{Te} + 0.5 \text{ wt. \% Te}$  and  $\text{Bi}_{0.5}\text{Sb}_{1.5}\text{Te} + 1.0 \text{ wt. \% Te}$ ) and  $n$ -type ( $\text{Pb}_{0.99}\text{In}_{0.01}\text{Te}$  and  $\text{PbTe}_{0.99}\text{In}_{0.01}$ ) films were prepared on a thin flexible polyimide substrate.

Figure 9a presents the Seebeck coefficient  $S$  for these films over the entire temperature range of 300 – 600 K. The temperature trend of the Seebeck

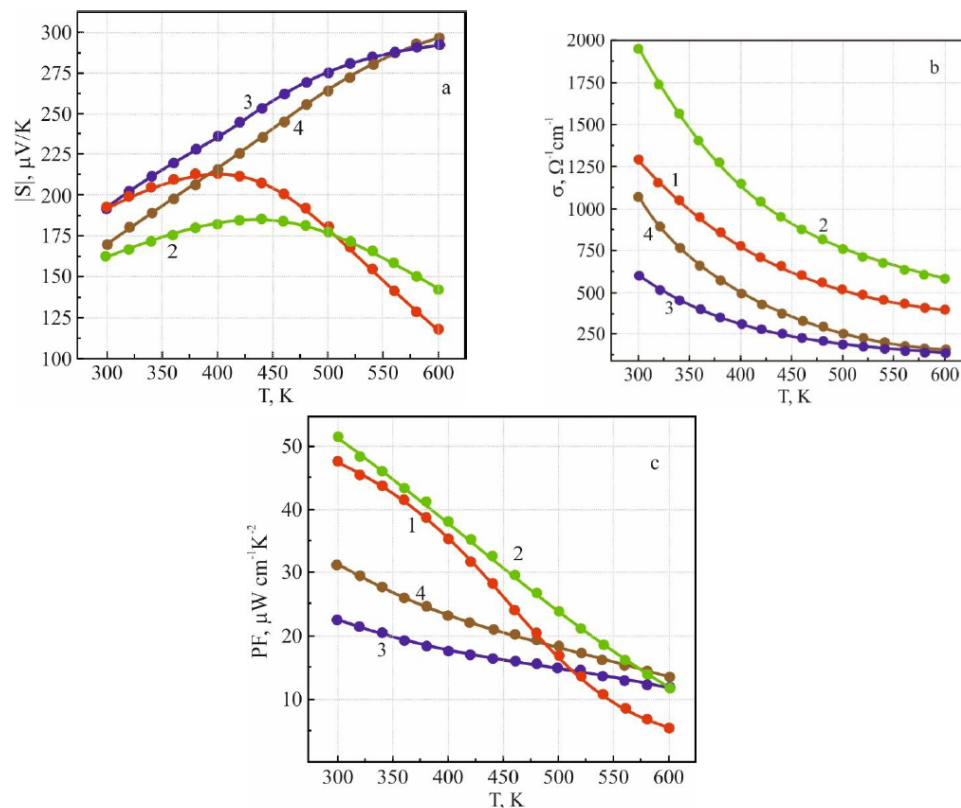


**Figure 9:** Temperature dependence of Seebeck coefficient  $S$  (absolute value) (a), electrical conductivity  $\sigma$  (b) and Power factor  $P = S^2\sigma$  (c) as a function of temperature for  $p$ - and  $n$ -type thermoelectric films prepared by flash evaporation.

1 -  $p$ -type  $\text{Bi}_{0.5}\text{Sb}_{1.5}\text{Te} + 1.0 \text{ wt. \% Te}$ . 2 -  $p$ -type  $\text{Bi}_{0.5}\text{Sb}_{1.5}\text{Te} + 0.5 \text{ wt. \% Te}$ . 3 -  $n$ -type  $\text{Pb}_{0.99}\text{In}_{0.01}\text{Te}$ . 4 -  $\text{PbTe}_{0.99}\text{In}_{0.01}$ .

coefficient for  $p$ -type films shows the maximum and then goes down due to the effect of intrinsic carriers, which is typical for narrow-band gap semiconductors.

Electrical conductivity of the investigated films decreases over the investigated temperature range indicating a metallic character (Figure 9b). Excellent thermoelectric performance of the fabricated films was confirmed by estimation of the Power Factor  $P = S^2\sigma$ . (Figure 9c). The maximum value was  $S^2\sigma \approx 50 \text{ W/cmK}$  at  $T = 300 \text{ K}$  for  $p$ -type films, which is practically equal to the power factor for the best bulk samples with the same chemical composition [11,28].

Table 2 presents measured thermoelectric characteristics (Seebeck coefficient  $S$ , electrical conductivity  $\sigma$  and thermal conductivity  $\kappa$ ) at  $T = 300 \text{ K}$  for  $p$ -type and  $n$ -type films of different compositions. The measurement method for  $S$ ,  $\sigma$  and  $\kappa$  are presented in our manuscript [35].

## 6.2. Solar Film Thermoelectric Module (FTEM) on Flexible Substrate

Fabrication of FTEM includes the following stages:

1. Preparation of  $p$ -type  $\text{Bi}_{0.5}\text{Sb}_{1.5}\text{Te}_3$  film legs with

the thickness of  $\sim 3 \mu\text{m}$  on both sides of the polyimide substrate ( $\sim 10 \mu\text{m}$ ).

2. Preparation of  $n$ -type  $\text{Pb}_{0.99}\text{In}_{0.01}\text{Te}$  film legs with the thickness of  $\sim 3 \mu\text{m}$  on both sides of the polyimide substrate.

3. Fabrication of perforations between  $p$ - and  $n$ -type legs. The size of the cut is  $\sim 0.2 \text{ mm}$  and the distance between the cuts is  $\sim 1 \text{ mm}$ .

4. Fabrication of electrical connection between the  $p$ - and  $n$ -type legs by Cr and Au layers with the thicknesses of  $0.1$  and  $1 \mu\text{m}$ , respectively, on both sides of the polyimide substrate and inside the perforation cuts.

5. Fabrication of a thin protective coating with the thickness of  $\sim 0.5 \mu\text{m}$  on both sides of the FTEM by plasma-chemical method of cyclohexane polymerization [73].

Schematic view of the main stages of fabrication of the flexible FTEM based on  $p\text{-Bi}_{0.5}\text{Sb}_{1.5}\text{Te}_3$  and  $n\text{-PbTe:In}$  thermoelectric materials is presented in Figure 10.

**Table 2: Thermoelectric Properties of  $p$ -Type  $\text{Bi}_{0.5}\text{Sb}_{1.5}\text{Te}_3$  and  $n$ -Type  $\text{PbTe:In}$  Films and Bulk Crystals at  $T = 300 \text{ K}$**

Composition	Type of material	Seebeck coefficient $S$ , $\mu\text{V/K}$	Electrical conductivity $\sigma$ , $\Omega^{-1}\text{cm}^{-1}$	Thermal conductivity $\kappa \times 10^3$ , $\text{W/cm.K}$	Figure of merit $Z \times 10^3$ , $\text{K}^{-1}$	Ref.
$\text{Bi}_{0.5}\text{Sb}_{1.5}\text{Te}_3 + 1.0 \text{ wt. \% Te}$	film	190	1250	15	3.0	
$\text{Pb}_{0.99}\text{In}_{0.01}\text{Te}$	film	-190	670	20	1.2	
$\text{Bi}_{0.5}\text{Sb}_{1.5}\text{Te}_3$	bulk	200	1150	16	3.0	[11]
$\text{Pb}_{0.999}\text{In}_{0.001}\text{Te}$	bulk	-200	600	23	1.1	[28]

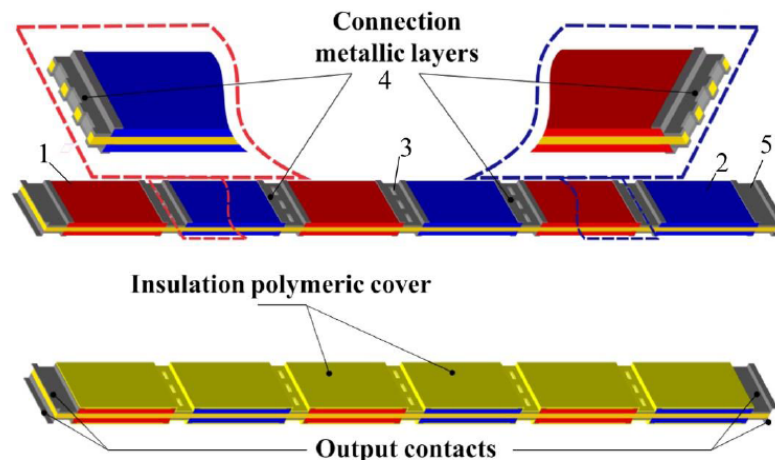


**Figure 10:** Schematic view of FTEM. a) - planar design. b) a view of the film module after protective coating.

1 -  $p$ -legs. 2 -  $n$ -legs. 3- perforation. 4 - metallic connecting layers between legs. 5 - output electric contacts.

### 6.3. Solar Application of FTEM

FTEM can be used for fabrication of film solar thermoelectric converter (generator). The principle of its operation may be described as follows: the incoming solar radiation creates a temperature gradient across FTEM, which generates electricity due to the thermoelectric effect. A schematic view of the proposed solar thermoelectric converter is presented in Figure 11. The electric voltage was induced by heating the hot side of the film thermoelectric unicouples. The cold side temperature of the film thermoelectric unicouples was stabilized by a black body with the temperature of 300 K.

The flexible polyimide substrate and perforation cuts between *p*- and *n*-legs allow to bend substrate along the perforation and to create a compact (packaged) design of the FTEM.

Such film thermoelectric converters with output voltage of several volts and electric power of several microwatts at the temperature of the hot side of FTEM  $T_h \sim 400$  K can be used in solar micro-energy systems.

### CONCLUSIONS

Due to the increase in energy demand and depletion of natural resources, the development of energy harvesting technologies becomes very important. High reliability and long operation time lead to a wide use of TEGs in space industry and gas pipe systems. Further development and wider application of solar TEGs is mainly limited by their relatively low conversion efficiencies. To overcome this issue, we suggest for the first time to use direct conversion of solar energy by a high-perfection thermoelectric

modules for creation of autonomic systems with electric power up to 500 W and electric efficiency up to 15 %.

To achieve this goal, unique multilayer (multistage) thermoelectric module was developed. Two types of high-efficiency thermoelectric materials were selected to ensure a wide range of operating temperatures.

The first type is the “low-temperature” thermoelectrics (300 - 600 K temperature range) based on  $\text{Bi}_2\text{Te}_3$  compounds (n-type solid solutions  $\text{Bi}_2\text{Te}_{3-x}\text{Se}_x$ , p-type solid solution  $\text{Bi}_{0.5}\text{Sb}_{1.5}\text{Te}_3$  with orientation along the crystal axis C, obtained by hot pressing in argon atmosphere.

The second type is the “middle-temperature” thermoelectrics (600 - 900 K temperature range) prepared by modern SPS technique. For the n-type thermoelectrics were used two stages – the first stage - classic PbTe doped by iodine and second stage - novel material PbTe doped by indium, creating the resonance level at the conduction band, which provided practically constant value of average figure of merit  $ZT$  at wide temperature range. Thermoelectrics of p-type were based on GeTe semiconductor compound doped by Bi up to 5 atomic %. It allowed to decrease the hole concentration to the values close to the optimal one from the point of view of TE efficiency ( $ZT$ ). On the other hand, this thermoelectrics had satisfactory mechanical properties, in contrast with high-efficiency p-type PbTe.

We developed for the first time film thermoelectric modules on thin flexible substrate with the values of figure of merit  $Z$  comparable to those of bulk modules. Such film thermoelectric converters with output voltage

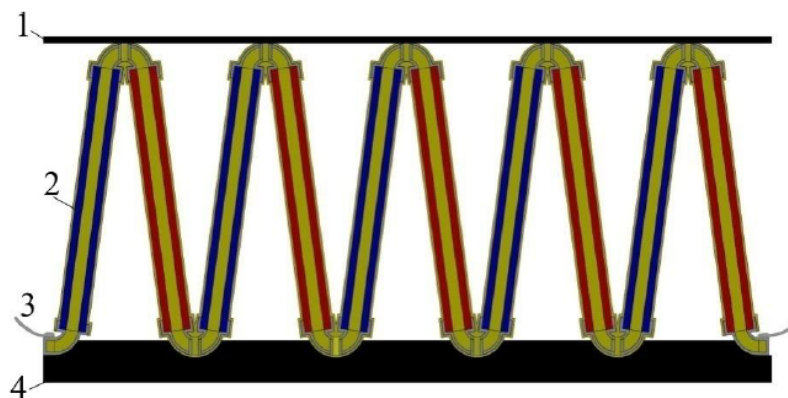


**Figure 11:** Schematic view of Solar Film Thermoelectric Converter (SFTEC).

1– absorption layer. 2– FTEM on flexible (polyimide) substrate. 3 – electric contacts. 4 – heat sink (black body).

of several volts and electric power of several microwatts can be used in solar micro-energy systems.

## AUTHOR CONTRIBUTIONS

S. Mamykin – Principal Investigator; I. Mamontova - Investigation, Calculations; B. Dzundza – Investigation and visualization; Feng Gao – Project Management and conceptualization; Z. Dashevsky – Supervision.

## FUNDING

This research received no external funding.

## CONFLICTS OF INTEREST

The authors declare that they have no known competing financial interests or personal relationships that could influence the work reported in this paper.

## REFERENCES

- [1] M.A. Zoui, S. Bentouba, J.G. Stocholm, M. Bourouis, A review on thermoelectric generators: Progress and applications, *Energies*, 13 (2020) 3606. <https://doi.org/10.3390/en13143606>
- [2] S.S. Indira, C.A. Vaithilingam, K.K. Chong, R. Saidur, M. Faizal, S. Abubakar, S. Paiman, A review on various configurations of hybrid concentrator photovoltaic and thermoelectric generator system, *Solar Energy*, 201 (2020) 122-148. <https://doi.org/10.1016/j.solener.2020.02.090>
- [3] Z. Dashevsky, P. Konstantinov, S.Y. Skipidarov, New Direction in the Application of Thermoelectric Energy Converters, *Semiconductors*, 53 (2019) 861-864. <https://doi.org/10.1134/S1063782619070066>
- [4] D. Champier, Thermoelectric generators: A review of applications, *Energy Conversion and Management*, 140 (2017) 167-181. <https://doi.org/10.1016/j.enconman.2017.02.070>
- [5] T.M. Maslamani, A.I. Omer, M. Majid, Development of solar thermoelectric generator, *European Scientific Journal*, 10 (2014).
- [6] Z. Dashevsky, D. Kaftori, D. Rabinovich, High efficiency thermoelectric unit within an autonomous solar energy converter, in: *Seventeenth International Conference on Thermoelectrics. Proceedings ICT98 (Cat. No. 98TH8365)*, IEEE, 1998, pp. 531-534.
- [7] H. Field, Solar cell spectral response measurement errors related to spectral band width and chopped light waveform, in: *Conference Record of the Twenty Sixth IEEE Photovoltaic Specialists Conference-1997*, IEEE, 1997, pp. 471-474.
- [8] G. Huang, S.R. Curt, K. Wang, C.N. Markides, Challenges and opportunities for nanomaterials in spectral splitting for high-performance hybrid solar photovoltaic-thermal applications: a review, *Nano Materials Science*, 2 (2020) 183-203. <https://doi.org/10.1016/j.nanoms.2020.03.008>
- [9] Z. Dashevsky, A. Jarashneli, Y. Unigovski, B. Dzundza, F. Gao, R.Z. Shneck, Development of a High Performance Gas Thermoelectric Generator (TEG) with Possible Use of Waste Heat, *Energies*, 15 (2022) 3960. <https://doi.org/10.3390/en15113960>
- [10] S. El Oualid, F. Kosior, A. Dauscher, C. Candolfi, G. Span, E. Mehmedovic, J. Paris, B. Lenoir, Innovative design of bismuth-telluride-based thermoelectric micro-generators with high output power, *Energy & Environmental Science*, 13 (2020) 3579-3591. <https://doi.org/10.1039/D0EE02579H>
- [11] Z. Dashevsky, S. Skipidarov, Investigating the performance of bismuth-antimony telluride, in: *Novel Thermoelectric Materials and Device Design Concepts*, Springer, 2019, pp. 3-21. [https://doi.org/10.1007/978-3-030-12057-3\\_1](https://doi.org/10.1007/978-3-030-12057-3_1)
- [12] M.K. Rad, A. Rezaia, M. Omid, A. Rajabipour, L. Rosendahl, Study on material properties effect for maximization of thermoelectric power generation, *Renewable energy*, 138 (2019) 236-242. <https://doi.org/10.1016/j.renene.2019.01.104>
- [13] H. Mamur, M. Bhuiyan, F. Korkmaz, M. Nil, A review on bismuth telluride (Bi<sub>2</sub>Te<sub>3</sub>) nanostructure for thermoelectric applications, *Renewable and Sustainable Energy Reviews*, 82 (2018) 4159-4169. <https://doi.org/10.1016/j.rser.2017.10.112>
- [14] M. Maksymuk, B. Dzundza, O. Matkivsky, I. Horichok, R. Shneck, Z. Dashevsky, Development of the high performance thermoelectric unicouple based on Bi<sub>2</sub>Te<sub>3</sub> compounds, *Journal of Power Sources*, 530 (2022) 231301. <https://doi.org/10.1016/j.jpowsour.2022.231301>
- [15] C. Gayner, K.K. Kar, Recent advances in thermoelectric materials, *Progress in Materials Science*, 83 (2016) 330-382. <https://doi.org/10.1016/j.pmatsci.2016.07.002>
- [16] J.R. Sootsman, D.Y. Chung, M.G. Kanatzidis, New and old concepts in thermoelectric materials, *Angewandte Chemie International Edition*, 48 (2009) 8616-8639. <https://doi.org/10.1002/anie.200900598>
- [17] Y. Gelbstein, Z. Dashevsky, M. Dariel, High performance n-type PbTe-based materials for thermoelectric applications, *Physica B: Condensed Matter*, 363 (2005) 196-205. <https://doi.org/10.1016/j.physb.2005.03.022>
- [18] T. Parashchuk, I. Horichok, A. Kosonowski, O. Cherniushok, P. Wyzga, G. Cempura, A. Kruk, K.T. Wojciechowski, Insight into the transport properties and enhanced thermoelectric performance of n-type Pb<sub>1-x</sub>Sb<sub>x</sub>Te, *Journal of Alloys and Compounds*, 860 (2021) 158355. <https://doi.org/10.1016/j.jallcom.2020.158355>
- [19] R. Knura, T. Parashchuk, A. Yoshiasa, K.T. Wojciechowski, Origins of low lattice thermal conductivity of Pb<sub>1-x</sub>Sn<sub>x</sub>Te alloys for thermoelectric applications, *Dalton Transactions*, 50 (2021) 4323-4334. <https://doi.org/10.1039/D0TD04206D>
- [20] I. Petsagkourakis, K. Tybrandt, X. Crispin, I. Ohkubo, N. Satoh, T. Mori, Thermoelectric materials and applications for energy harvesting power generation, *Science and technology of advanced materials*, 19 (2018) 836-862. <https://doi.org/10.1080/14686996.2018.1530938>
- [21] T. Parashchuk, A. Shabaldin, O. Cherniushok, G. Konstantinov, I. Horichok, A. Burkov, Z. Dashevsky, Enhanced thermoelectric properties of p-type Ge<sub>1-x</sub>Pb<sub>x</sub>Te alloys due to decrease of lattice thermal conductivity, *J. Physica B.*, 596 (2020) 412397. <https://doi.org/10.1016/j.physb.2020.412397>
- [22] K. Romanjek, S. Vesin, L. Aixala, T. Baffie, G. Bernard-Granger, J. Dufourcq, High-performance silicon-germanium-based thermoelectric modules for gas exhaust energy scavenging, *Journal of Electronic Materials*, 44 (2015) 2192-2202. <https://doi.org/10.1007/s11664-015-3761-1>
- [23] K. Delime-Codrin, M. Omprakash, S. Ghodke, R. Sobota, M. Adachi, M. Kiyama, T. Matsuura, Y. Yamamoto, M. Matsunami, T. Takeuchi, Large figure of merit ZT= 1.88 at 873 K achieved with nanostructured Si<sub>0.55</sub>Ge<sub>0.35</sub>(P<sub>0.10</sub>Fe<sub>0.01</sub>), *Applied Physics Express*, 12 (2019) 045507. <https://doi.org/10.7567/1882-0786/ab08b7>

- [24] O. Ben-Yehuda, R. Shuker, Y. Gelbstein, Z. Dashevsky, M. Dariel, Highly textured Bi<sub>2</sub>Te<sub>3</sub>-based materials for thermoelectric energy conversion, *Journal of Applied Physics*, 101 (2007) 113707. <https://doi.org/10.1063/1.2743816>
- [25] DB. Hyun, JS. Hwang, JD. Shim, TS. Oh, Thermoelectric properties of (Bi<sub>0.25</sub>Sb<sub>0.75</sub>)<sub>2</sub>Te<sub>3</sub> alloys fabricated by hot-pressing method, *Journal of materials science*, 36 (2001) 1285-1291.
- [26] J. Mi, T. Zhu, X. Zhao, J. Ma, Nanostructuring and thermoelectric properties of bulk skutterudite compound CoSb<sub>3</sub>, *Journal of Applied Physics*, 101 (2007) 054314. <https://doi.org/10.1063/1.2436927>
- [27] O. Ben-Yehuda, Y. Gelbstein, Z. Dashevsky, Y. George, M. Dariel, Functionally Graded Bi<sub>2</sub>Te<sub>3</sub> based material for above ambient temperature application, in: 2007 26th International Conference on Thermoelectrics, IEEE, 2007, pp. 82-85.
- [28] T. Parashchuk, Z. Dashevsky, K. Wojciechowski, Feasibility of a high stable PbTe: In semiconductor for thermoelectric energy applications, *Journal of Applied Physics*, 125 (2019) 245103. <https://doi.org/10.1063/1.5106422>
- [29] K.T. Wojciechowski, T. Parashchuk, B. Wiendlocha, O. Cherniushok, Z. Dashevsky, Highly efficient n-type PbTe developed by advanced electronic structure engineering, *Journal of Materials Chemistry C*, 8 (2020) 13270-13285. <https://doi.org/10.1039/D0TC03067H>
- [30] B. Srinivasan, R. Gautier, F. Gucci, B. Fontaine, J.-F. Halet, F. Chev r , C. Boussard-Pl del, M.J. Reece, B. Bureau, Impact of coinage metal insertion on the thermoelectric properties of GeTe solid-state solutions, *The Journal of Physical Chemistry C*, 122 (2018) 227-235. <https://doi.org/10.1021/acs.jpcc.7b10839>
- [31] Z. Dashevsky, I. Horichok, M. Maksymuk, A.R. Muchtar, B. Srinivasan, T. Mori, Feasibility of high performance in p-type Ge<sub>1-x</sub>Bi<sub>x</sub>Te materials for thermoelectric modules, *Journal of the American Ceramic Society*, 105 (2022) 4500-4511. <https://doi.org/10.1111/jace.18371>
- [32] O. Kostyuk, B. Dzunza, M. Maksymuk, V. Bublik, L. Chernyak, Z. Dashevsky, Development of Spark Plasma Sintering (SPS) technology for preparation of nanocrystalline p-type thermoelectrics based on (BiSb)<sub>2</sub>Te<sub>3</sub>, *Physics and Chemistry of Solid State*, 21 (2020) 628-634. <https://doi.org/10.15330/pccs.21.4.628-634>
- [33] B.M. Goltsman, Z. Dashevsky, V. Kaydanov, N. Kolomoets, Thin films: Physics and application, Nauka, 1986.
- [34] T. Parashchuk, O. Kostyuk, L. Nykyruy, Z. Dashevsky, High thermoelectric performance of p-type Bi<sub>0.5</sub>Sb<sub>1.5</sub>Te<sub>3</sub> films on flexible substrate, *Materials Chemistry and Physics*, 253 (2020) 123427. <https://doi.org/10.1016/j.matchemphys.2020.123427>
- [35] B. Dzunza, L. Nykyruy, T. Parashchuk, E. Ivakin, Y. Yavorsky, L. Chernyak, Z. Dashevsky, Transport and thermoelectric performance of n-type PbTe films, *Physica B: Condensed Matter*, 588 (2020) 412178. <https://doi.org/10.1016/j.physb.2020.412178>
- [36] J. Seo, C. Lee, K. Park, Thermoelectric properties of n-type Sb<sub>13</sub>-doped Bi<sub>2</sub>Te<sub>2.85</sub>Se<sub>0.15</sub> compound fabricated by hot pressing and hot extrusion, *Journal of materials science*, 35 (2000) 1549-1554.
- [37] N. Bomshtein, G. Spiridonov, Z. Dashevsky, Y. Gelbstein, Thermoelectric, structural, and mechanical properties of spark-plasma-sintered submicro-and microstructured p-type Bi<sub>0.5</sub>Sb<sub>1.5</sub>Te<sub>3</sub>, *Journal of Electronic Materials*, 41 (2012) 1546-1553. <https://doi.org/10.1007/s11664-012-1950-8>
- [38] L. Prokofieva, D. Pshenay-Severin, P. Konstantinov, A. Shabaldin, Optimum composition of a Bi<sub>2</sub>Te<sub>3</sub>- xSex alloy for the n-type leg of a thermoelectric generator, *Semiconductors*, 43 (2009) 973-976. <https://doi.org/10.1134/S1063782609080016>
- [39] I.T. Witting, F. Ricci, T.C. Chasapis, G. Hautier, G.J. Snyder, The thermoelectric properties of-type bismuth telluride: bismuth selenide alloys, *Research*, 2020 (2020) 1-15. <https://doi.org/10.34133/2020/4361703>
- [40] V. Kaifanov, Y.I. Ravich, Deep and resonance states in AIVBVI semiconductors, *Soviet Physics Uspekhi*, 28 (1985) 31. <https://doi.org/10.1070/PU1985v028n01ABEH003632>
- [41] V. Kaidanov, Resonance (Quasilocal) states in AIVBVI semiconductors, in: *Defect and Diffusion Forum*, Trans Tech Publ, 1993, pp. 387-406. <https://doi.org/10.4028/www.scientific.net/DDF.103-105.387>
- [42] Z. Dashevsky, S. Shusterman, M. Dariel, I. Drabkin, Thermoelectric efficiency in graded indium-doped PbTe crystals, *Journal of Applied Physics*, 92 (2002) 1425-1430. <https://doi.org/10.1063/1.1490152>
- [43] J.P. Heremans, B. Wiendlocha, A.M. Chamoire, Resonant levels in bulk thermoelectric semiconductors, *Energy & Environmental Science*, 5 (2012) 5510-5530. <https://doi.org/10.1039/C1EE02612G>
- [44] A. Bali, R. Chetty, A. Sharma, G. Rogl, P. Heinrich, S. Suwas, D.K. Misra, P. Rogl, E. Bauer, R.C. Mallik, Thermoelectric properties of In and I doped PbTe, *Journal of Applied Physics*, 120 (2016) 175101. <https://doi.org/10.1063/1.4965865>
- [45] J. Androulakis, I. Todorov, D.-Y. Chung, S. Ballikaya, G. Wang, C. Uher, M. Kanatzidis, Thermoelectric enhancement in PbTe with K or Na codoping from tuning the interaction of the light-and heavy-hole valence bands, *Physical Review B*, 82 (2010) 115209. <https://doi.org/10.1103/PhysRevB.82.115209>
- [46] P. Jood, J.P. Male, S. Anand, Y. Matsushita, Y. Takagiwa, M.G. Kanatzidis, G.J. Snyder, M. Ohta, Na doping in PbTe: solubility, band convergence, phase boundary mapping, and thermoelectric properties, *Journal of the American Chemical Society*, 142 (2020) 15464-15475. <https://doi.org/10.1021/jacs.0c07067>
- [47] T. Parashchuk, B. Wiendlocha, O. Cherniushok, R. Knura, K.T. Wojciechowski, High thermoelectric performance of p-type PbTe enabled by the synergy of resonance scattering and lattice softening, *ACS Applied Materials & Interfaces*, 13 (2021) 49027-49042. <https://doi.org/10.1021/acsami.1c14236>
- [48] M. Dariel, Z. Dashevsky, A. Jarashnely, S. Shusterman, A. Horowitz, Carrier concentration gradient generated in p-type PbTe crystals by unidirectional solidification, *Journal of crystal growth*, 234 (2002) 164-170. [https://doi.org/10.1016/S0022-0248\(01\)01660-8](https://doi.org/10.1016/S0022-0248(01)01660-8)
- [49] J.P. Male, L. Abdellaoui, Y. Yu, S. Zhang, N. Pieczulewski, O. Cojocar-Mir din, C. Scheu, G.J. Snyder, Dislocations stabilized by point defects increase brittleness in PbTe, *Advanced Functional Materials*, 31 (2021) 2108006. <https://doi.org/10.1002/adfm.202108006>
- [50] Y. Gelbstein, G. Gotesman, Y. Lishzinker, Z. Dashevsky, M. Dariel, Mechanical properties of PbTe-based thermoelectric semiconductors, *Scripta Materialia*, 58 (2008) 251-254. <https://doi.org/10.1016/j.scriptamat.2007.10.012>
- [51] Y. Gelbstein, Z. Dashevsky, M.P. Dariel, The search for mechanically stable PbTe based thermoelectric materials, *Journal of Applied Physics*, 104 (2008) 033702. <https://doi.org/10.1063/1.2963359>
- [52] Z. Dashevsky, L. Dudkin, Generator thermoelectric materials, *J. Thermoelectricity*, 1 (1993) 93-99.
- [53] A. Faghri, Heat pipes: review, opportunities and challenges, *Frontiers in Heat Pipes (FHP)*, 5 (2014). <https://doi.org/10.5098/fhp.5.1>

- [54] S. El Oualid, I. Kogut, M. Benyahia, E. Geczi, U. Kruck, F. Kosior, P. Masschelein, C. Candolfi, A. Dauscher, J.D. Koenig, High Power Density Thermoelectric Generators with Skutterudites, *Advanced Energy Materials*, 11 (2021) 2100580.  
<https://doi.org/10.1002/aenm.202100580>
- [55] A.P. Raman, M.A. Anoma, L. Zhu, E. Rephaeli, S. Fan, Passive radiative cooling below ambient air temperature under direct sunlight, *Nature*, 515 (2014) 540-544.  
<https://doi.org/10.1038/nature13883>
- [56] S.V. Boriskina, M.A. Green, K. Catchpole, E. Yablonovitch, M.C. Beard, Y. Okada, S. Lany, T. Gershon, A. Zakutayev, M.H. Tahersima, Roadmap on optical energy conversion, *Journal of Optics*, 18 (2016) 073004.  
<https://doi.org/10.1088/2040-8978/18/7/073004>
- [57] S.V. Boriskina, J.K. Tong, W.-C. Hsu, B. Liao, Y. Huang, V. Chiloyan, G. Chen, Heat meets light on the nanoscale, *Nanophotonics*, 5 (2016) 134-160.  
<https://doi.org/10.1515/nanoph-2016-0010>
- [58] M.I. Stockman, K. Kneipp, S.I. Bozhevolnyi, S. Saha, A. Dutta, J. Ndukaife, N. Kinsey, H. Reddy, U. Guler, V.M. Shalaev, Roadmap on plasmonics, *Journal of Optics*, 20 (2018) 043001.  
<https://doi.org/10.1088/2040-8986/aaa114>
- [59] W. Xie, Y. Dai, R. Wang, K. Sumathy, Concentrated solar energy applications using Fresnel lenses: A review, *Renewable and Sustainable Energy Reviews*, 15 (2011) 2588-2606.  
<https://doi.org/10.1016/j.rser.2011.03.031>
- [60] A. Pfahl, J. Coventry, M. Röger, F. Wolfertstetter, J.F. Vázquez-Arango, F. Gross, M. Arjomandi, P. Schwarzbözl, M. Geiger, P. Liedke, Progress in heliostat development, *Solar Energy*, 152 (2017) 3-37.  
<https://doi.org/10.1016/j.solener.2017.03.029>
- [61] L. Li, X. Gao, G. Zhang, W. Xie, F. Wang, W. Yao, Combined solar concentration and carbon nanotube absorber for high performance solar thermoelectric generators, *Energy Conversion and Management*, 183 (2019) 109-115.  
<https://doi.org/10.1016/j.enconman.2018.12.104>
- [62] H.K. Raut, V.A. Ganesh, A.S. Nair, S. Ramakrishna, Anti-reflective coatings: A critical, in-depth review, *Energy & Environmental Science*, 4 (2011) 3779-3804.  
<https://doi.org/10.1039/c1ee01297e>
- [63] G.J. Snyder, J.R. Lim, C.K. Huang, and J.P. Fleurial, Thermoelectric microdevice fabricated by a MEMS-like electrochemical process. *Nature materials* 2, 528 (2003).  
<https://doi.org/10.1038/nmat943>
- [64] M. Takashiri, T. Shirakawa, K. Miyazaki, H. Tsukamoto. Fabrication and characterization by bismuth - telluride - based alloy thin-film thermoelectric generators by a flash evaporation method. *Sens. Actuators A* 138, 329 (2007).  
<https://doi.org/10.1016/j.sna.2007.05.030>
- [65] J. Kurosaki, A. Yamamoto, S. Tanaka, J. Cannon, K. Miyazaki, and H. Tsukamoto. Fabrication and Evaluation of a Thermoelectric Microdevice on a Free-Standing Substrate. *J. Electron. Mater.* 38, 1326 (2009).  
<https://doi.org/10.1007/s11664-009-0819-y>
- [66] P. Fan, Z. Zheng, V. Li, G. Lin. Low-cost flexible thin-film thermoelectric generator on zinc-based thermoelectric material. *Appl. Phys. Lett.* 106, 073901 (2015).  
<https://doi.org/10.1063/1.4909531>
- [67] M. Takashiri, T. Shirakawa, K. Miyazaki, and H. Tsukamoto, Fabrication and characterization of bismuth-telluride-based alloy thin-film thermoelectric generators by a flash evaporation method. *Sens. Actuators A Phys.* 138 (2007) 329-334.  
<https://doi.org/10.1016/j.sna.2007.05.030>
- [68] P. Fan, Z.-H. Zheng, Z.-K. Cai, T.-B. Chen, P.-J. Liu, X.-M. Cai, D.-P. Zhang, G.-X. Liang, and J.-T. Luo, The high performance of a thin-film thermoelectric generator with heat flow running parallel to film surface, *Appl. Phys. Lett.* 102, 033904 (2013).  
<https://doi.org/10.1063/1.4788817>
- [69] M. Mizoshiri, M. Makami, K. Ozaki, K. Kozayashi. Thin-Film Thermoelectric Modules for Power Generation Using Focused Solar Light. *J. of Elect. Mat.* 41, 1717 (2012).  
<https://doi.org/10.1007/s11664-012-2047-0>
- [70] K. Tappura, K. Jaakkola. A Thin-Film Thermoelectric Generator for Large Area Applications. *Proceeding 2*, 779 (2018).  
<https://doi.org/10.3390/proceedings2130779>
- [71] P. Fan, Z. Zheng, Z. Cai, T. Chen, P. Liu, The high performance of a thin-film thermoelectric generator with heat flow running parallel to film surface, *Appl. Phys. Lett.*, 102 (2013).  
<https://doi.org/10.1063/1.4788817>
- [72] M. Maksymuk, T. Parashchuk, B. Dzundza, L. Nykyryu, L. Chernyak, Z. Dashevsky. Development of the flexible film thermoelectric microgenerator based on Bi<sub>2</sub>Te<sub>3</sub> alloys. *J. Materials Today Energy*. (2021).
- [73] O. Kostyuk, Ya. Yavorsky, B. Dzundza, Z. Dashevsky. Development of thermal detector based on flexible film thermoelectric module. *J. Physics and Chemistry of Solid State*. 22, 45 (2021).  
<https://doi.org/10.15330/pcss.22.1.45-52>

Received on 06-07-2022

Accepted on 11-08-2022

Published on 29-08-2022

DOI: <https://doi.org/10.31875/2410-2199.2022.09.05>© 2022 Mamykin *et al.*; Zeal Press.

This is an open access article licensed under the terms of the Creative Commons Attribution License

[\(http://creativecommons.org/licenses/by/4.0/\)](http://creativecommons.org/licenses/by/4.0/) which permits unrestricted use, distribution and reproduction in any medium, provided the work is properly cited.